Neurobiology of Disease 105 (2017) 1–14

Contents lists available at ScienceDirect

Neurobiology of Disease

journal homepage: www.elsevier.com/locate/ynbdi

Gene co-expression networks identify *Trem2* and *Tyrobp* as major hubs in human APOE expressing mice following traumatic brain injury

Emilie L. Castranio [a], Anais Mounier [a], Cody M. Wolfe [a], Kyong Nyon Nam [a], Nicholas F. Fitz [a], Florent Letronne [a], Jonathan Schug [b], Radosveta Koldamova [a,*], Iliya Lefterov [a,*]

[a] Department of Environmental and Occupational Health, University of Pittsburgh, Pittsburgh, PA 15219, USA
[b] Functional Genomics Core, Department of Genetics, University of Pennsylvania, Philadelphia, PA 19104, USA

ARTICLE INFO

Article history:
Received 3 January 2017
Revised 1 May 2017
Accepted 10 May 2017
Available online 11 May 2017

Keywords:
Apolipoprotein E
Traumatic brain injury
Trem2
Tyrobp
Myelination
Immune response
Fyn
Innate immune response

ABSTRACT

Traumatic brain injury (TBI) is strongly linked to an increased risk of developing dementia, including chronic traumatic encephalopathy and possibly Alzheimer's disease (AD). *APOEε4* allele of human Apolipoprotein E (*APOE*) gene is the major genetic risk factor for late onset AD and has been associated with chronic traumatic encephalopathy and unfavorable outcome following TBI. To determine if there is an APOE isoform-specific response to TBI we performed controlled cortical impact on 3-month-old mice expressing human APOE3 or APOE4 isoforms. Following injury, we used several behavior paradigms to test for anxiety and learning and found that APOE3 and APOE4 targeted replacement mice demonstrate cognitive impairments following moderate TBI. Transcriptional profiling 14 days following injury revealed a significant effect of TBI, which was similar in both genotypes. Significantly upregulated by injury in both genotypes were mRNA expression and protein level of ABCA1 transporter and APOJ, but not APOE.

To identify gene-networks correlated to injury and APOE isoform, we performed Weighted Gene Co-expression Network Analysis. We determined that the network mostly correlated to TBI in animals expressing both isoforms is immune response with major hub genes including *Trem2*, *Tyrobp*, *Clec7a and Cd68*. We also found a significant increase of TREM2, IBA-1 and GFAP protein levels in the brains of injured mice. We identified a network representing myelination that correlated significantly with APOE isoform in both injury groups. This network was significantly enriched in oligodendrocyte signature genes, such as *Mbp* and *Plp1*. Our results demonstrate unique and distinct gene networks at this acute time point for injury and APOE isoform, as well as a network driven by APOE isoform across TBI groups.

1. Introduction

Traumatic brain injury (TBI) is one of the leading causes of death and disability in the United States. Approximately 2 million people sustain a TBI and 50,000 TBI-related deaths occur in the United States every year. Currently, there is no treatment for TBI, patients are only given supportive care for which the cost is approximately $60 billion annually. TBI can either be caused when the head violently impacts with another object or when an object pierces the skull and enters the brain tissue. Studies show that following the acute phase, over the long-term, patients may develop changes in cognition, and increases in both anxiety and depression (Perez-Garcia et al., 2016; Ghroubi et al., 2016). The high level of variability in injury outcomes suggests, to a significant extent, a strong role for genetic influence on brain susceptibility and recovery (Draper and Ponsford, 2008; Whitnall et al., 2006).

TBI is strongly linked to increased risk of developing dementia, including chronic traumatic encephalopathy and possibly Alzheimer's disease (AD) (Jordan, 2007; Jordan, 2014; McKee et al., 2016). The *APOEε4* allele of human apolipoprotein E (*APOE*) gene is the major genetic risk factor for late onset AD and has been associated with chronic traumatic encephalopathy and unfavorable outcome following TBI. Multiple studies have identified worse outcomes following TBI based on the inheritance of *APOEε4* allele (Alexander et al., 2007; Diaz-Arrastia et al., 2003). The role of APOE in neuronal survival and repair and in overall response to TBI, however, is not well understood. It has been suggested that APOE4 is less stable and catabolically degraded more quickly than the other APOE isoforms, possibly due to its lower lipidation level (Kim et al., 2009). In mice, studies have identified APOE-genotype and brain-region specific genomic changes using mRNA microarrays after controlled cortical impact (CCI) (Crawford et al., 2009). Patients, carriers of *APOEε4*, experiencing TBI demonstrated worse memory performance

* Corresponding authors at: Department of Environmental & Occupational Health, University of Pittsburgh, 100 Technology Dr., BRIDG Building, Pittsburgh, PA 15219, USA.
E-mail addresses: radak@pitt.edu (R. Koldamova), iliyal@pitt.edu (I. Lefterov).

http://dx.doi.org/10.1016/j.nbd.2017.05.006
0969-9961/

in a verbal learning test and verbal fluency measured 6 months post-injury (Crawford et al., 2002). In contrast, other in vivo data did not find or confirm a role for APOE4 in TBI (Mannix et al., 2011; Mannix et al., 2016; Moran et al., 2009; Willemse-van Son et al., 2008). For example, in adult patients with moderate to severe TBI assessed 3, 6 and 12 months post-injury, APOE4 patients did not have poorer cognitive performance, functional outcome or slower improvement (Ponsford et al., 2008). There is a uniform agreement that more studies are needed to clarify the role of *APOEε4* allele in TBI. Mechanical stress placed on the brain due to the impact is considered the primary injury. Following the impact, a secondary injury occurs leading to additional damage and cell death, worsening the outcome. Mechanisms of secondary injury include neuronal excitotoxicity, edema, oxidative stress, and neuroinflammation. The inflammatory state in the brain can persist for many years following the injury; chronic neuroinflammation following TBI was closely associated with neuronal death and impaired cell proliferation both immediately adjacent to, and locations more distant from, site of injury (Acosta et al., 2013). Multiple inflammatory molecules are upregulated after TBI and are believed to contribute to these processes, as well as blood brain barrier dysfunction. Interleukin-1β (IL-1β), tumor necrosis factor-α (TNF-α), chemokine C motif ligand 2 (Ccl2), and chemokine CX3C motif receptor 1 (Cx3cr1) are among those that have been intensely studied for their impact on brain pathology following TBI (Dalgard et al., 2012; Ferreira et al., 2014; Gyoneva and Ransohoff, 2015; Hua et al., 2011). Studies have shown that the expression levels of the majority of those inflammatory factors are associated with severity of injury and outcome in TBI patients, the reduction of neurobehavioral impairments and injury volume as well as the survival rates in rodent models (Morganti et al., 2015; Yang et al., 2013).

To our knowledge, transcription profiling of APOE expressing mice following TBI using Next Generation Sequencing has not yet been performed. The aim of this study was to determine if there is an interaction between APOE isoform and the response to TBI affecting phenotype and the transcriptome. We performed controlled cortical impact on 3-month-old mice expressing human APOE3 or APOE4 isoform and following the injury, tested for anxiety and learning. Transcriptional profiling of hippocampal and cortical tissue from the injury site was performed using mRNA-sequencing (mRNA-seq). We hypothesized that there is APOE isoform-specific response to injury and APOE4 mice would have worse cognitive outcomes and higher inflammatory gene expression following TBI. We found that APOE genotype, while a significant variable in both behavioral tests, did not modulate the changes in transcriptome seen two weeks post injury. To correlate the transcriptome to the phenotype we used network-based approach and applied Weighted Gene Co-expression Network Analysis (WGCNA). This analysis not only connects the genes within networks and identifies the most connected members of a given pathway, but elucidates the relevance of the networks to the experimental findings. Thus, we identified that TBI significantly affected immune response, with *Trem2* and *Tyrobp* being highly ranked within the interconnected gene network.

2. Methods

2.1. Animals

All animal experiments were approved through the University of Pittsburgh Institutional Animal Care and Use Committee and carried out in accordance with PHS policies on the use of animals in research. We used human APOE4$^{+/+}$ and APOE3$^{+/+}$ targeted replacement mice on a C57BL/6 background (Fitz et al., 2012). Experimental male and female APOE3 or APOE4 mice were kept on a 12 h light-dark cycle with ad libitum access to food and water. Mice at 3 months of age were randomly assigned to either sham or controlled cortical impact (CCI) experimental group and initially were handled for 2 days (5 min per day). Following surgical procedures, mice were allowed to recover for 3 days before starting behavioral testing. All materials were purchased through Thermo Fisher Scientific, unless otherwise noted.

2.2. Controlled cortical impact

CCI model of brain injury was performed according to previous published methods (Brody et al., 2007). Following induction of anesthesia with 5% isoflurane, the mouse was moved to the stereotaxic frame, where the head was secured, core body temperature maintained at 37 °C using a heating pad and anesthesia continued with 1.5% isoflurane. The head was shaven, surgical site sterilized with two separate iodine - alcohol washes, a 50% mixture of bupivacaine and lidocaine applied to the surgical site and ophthalmic ointment applied to the eyes. The scalp was opened with a midline incision exposing the dorsal aspect of the skull and the skull leveled. A 4.5 mm diameter craniotomy was performed over the left parietal cortex using a dental drill. Once the bone flap was removed, mice in the CCI group received a single impact at 1.0 mm depth with a 3.0 mm diameter metal tip onto the cortex (3 m/s, 100 ms dwell time; Impact One, Leica). Sham mice received identical anesthesia and craniotomy, but did not receive impact and are considered negative controls. Following the impact, the surgical site was sutured, triple antibiotic cream applied, Buprenex (0.1 mg/kg; IP) provided for analgesia, and sterile saline administered for rehydration. Mice were allowed to recover on heating pad, until freely mobile, before returning to their home cage.

2.3. Elevated-plus maze

The elevated plus maze (EPM, San Diego Instruments) test was performed 4 days post-injury as described previously (Washington et al., 2012). The maze consists of 4 arms in the shape of a "+". All arms are the same length (30.5 cm) with a central square (10 × 10 cm); 2 arms are open on the sides, and 2 have 16 cm high walls. The entire maze is raised 40 cm off the ground. The elevated plus maze tests anxiety-related behavior by utilizing rodent's fear of open and elevated spaces. Mice are placed into the maze within the center square facing a closed arm and are allowed to explore for 5 min. Percent time spent in each arm was tracked using the ANY-maze software (Stoelting Co.) from a camera positioned over the maze. 50% of body area within an arm was established in ANY-maze for definition of entry.

2.4. Morris water maze

Spatial navigational learning and memory retention were assessed using Morris water maze (MWM) as described previously (Fitz et al., 2010; Lefterov et al., 2010); with testing performed on days 6–12 post-injury. Briefly, in a circular pool of water (diameter 122 cm, height 51 cm, temperature 21 ± 1 °C), we measured the ability of mice to form a spatial relationship between a safe but invisible platform (submerged 1 cm below the water level; 10 cm in diameter) and several visual extra maze cues surrounding the pool of water. On day 6 post-injury, mice received a habituation trial, during which the animals were allowed to explore the pool of water without the platform present. Beginning the next day, they received four daily hidden platform training (acquisition) trials with 5-min inter-trial intervals for five consecutive days (days 7–11 post-injury). The platform remained in the center of one of the four quadrants of the pool (target quadrant). Animals were allowed 60 s to locate the platform and 20 s to remain there. Mice that failed to find the platform were lead to the platform by the experimenter and allowed to rest there for 20 s. Performance was recorded using Any-maze software (Stoelting Co.) during all trials. During the acquisition trials, escape latency (time to reach the platform) was subsequently used to analyze and compare the performance between all groups.

2.5. Animal tissue processing

Fourteen days post-injury, mice were anesthetized using Avertin (250 mg/kg of body weight, i.p.) and perfused transcardially with 20 ml of cold 0.1 M PBS pH 7.4, following a blood draw from the right atrium (Nam et al., 2016). Brains were rapidly removed and a 1.5 mm coronal section of the brain, including the injury site, was taken by slicing the brain at −2.5 mm and −4.0 from bregma. Within the coronal slice, the hemispheres were separated, and the subcortical tissue was dissected out; hippocampal and cortical tissue were snap-frozen together for mRNA-seq and RT-qPCR analysis. The remaining anterior of the brain was fixed in formalin for immunohistochemistry.

2.6. Immunohistochemistry

All procedures were as reported previously (Fitz et al., 2015; Jay et al., 2015; Savage et al., 2015). Briefly, OCT-embedded hemibrains were cut in the coronal plane at 20 μm sections and stored in a glycol-based cryoprotectant at −20 °C. Five sections starting at −0.20 from Bregma, separated by 500 μm were used for staining. Sections were washed in PBS and antigen retrieval performed with Reveal Decloaker at 100 °C for 30 min in a water bath. Quenching of endogenous peroxidases, blocking with 5% normal donkey serum and avidin-biotin blocking followed antigen retrieval. Sections were incubated in TREM2 primary antibody (1:100, AF179, R&D Systems) overnight at 4 °C, followed by washing in PBS and labeling with biotinylated secondary antibody (1:1000, donkey α sheep; A16045) and developed with Vectastain ABC Elite kit (Vector Laboratories) and DAB substrate. Sections for GFAP and Iba1 staining were blocked in 5% serum of the requisite host and incubated in primary antibody overnight (anti-GFAP: 1:1000, Z0334, Dako; Iba1: 1:200, 19–19741, WAKO). Secondary antibodies with conjugated fluorophores were applied as appropriate. Sections were mounted on charged slides and coverslipped with Permount. All slides were examined using the Nikon Eclipse 90i at 10× magnification and percent positive staining was defined as the percent area covered by staining using NIS Elements software (Nikon Instruments Inc.). The percent positive staining was determined by setting a threshold within the software. The threshold was determined using negative and positive controls to identify only stained tissue. Once set, the threshold was applied to all sections and then the ipsilateral and contralateral hemispheres were traced separately to identify the area. The software then calculates the amount of staining per area. Unless otherwise stated, analysis was conducted for ipsilateral hemispheres only. Contralateral hemispheres were identified using a pinhole made before sectioning.

2.7. RNA isolation and mRNA sequencing

All procedures were performed as before (Nam et al., 2016). Four APOE3 and APOE4 male and female mice per sham and CCI injured group were used for mRNA-seq. RNA was isolated from frozen cortices and hippocampi at the injury site and purified using RNeasy kit (Qiagen) according to the manufacturer recommendations. Quality control of all RNA samples was performed on a 2100 Bioanalyzer instrument and samples with RIN > 8 were further used for library construction using mRNA Library Prep Reagent Set (Illumina). Libraries were generated by PCR enrichment including incorporation of barcodes to enable multiplexing. The libraries, were sequenced on Illumina HiSeq2000. For RT-qPCR, first strand cDNA was synthesized from 1 μg of total RNA using EcoDry™ Premix, Random Hexamers (Clontech). Next Generation Sequencing of libraries was performed by the Next Generation Sequencing Center (University of Pennsylvania, http://fgc.genomics.upenn.edu/) on *HiSeq 2500* machine. Following initial processing and quality control, the sequencing datasets were further analyzed for differential gene expression, which in all cases was calculated using Subread/featureCounts (v1.5.0; https://sourceforge.net/projects/subread/files/subread-1.5.0/) for read alignment and summarization and statistical package edgeR (v3.14.0; https://bioconductor.org/packages/release/bioc/html/edgeR.html). Lists of differentially expressed genes are further analyzed as described in the following section.

2.8. Principle component analysis

Principle component analysis (PCA) was performed to determine the principle components, which account for the highest sources of variance in the dataset, using R (v. 3.3.2) packages and visualized using "ggbiplot2" (v2.1.0, https://github.com/vqv/ggbiplot) (Venables and Ripley, 2002).

2.9. Functional pathway analysis

We performed functional annotation clustering using the Database for Annotation, Visualization and Integrated Discovery (DAVID, http://david.abcc.ncifcrf.gov/version6.7) and Gene set enrichment Analysis (GSEA, v2.2.2, https://www.broadinstitute.org/GSEA) (Mootha et al., 2003; Subramanian et al., 2005).

2.10. Weighted Gene Co-expression Network Analysis

Network analysis was performed using WGCNA (v.1.49) (Zhao et al., 2010). Libraries are clustered by gene expression enabling the detection of outliers and the power is determined by scale free topology model. Modules were generated automatically using a soft thresholding power, $\beta = 10$, a minimum module size of 33 genes and a minimum module merge cut height of 0.25. Modules were named by conventional colour scheme and then correlated with trait data (APOE isoform, Injury). Each trait was converted individually into a binary factor, (e.g. Sham = 0, TBI = 1; APOE3 = 0, APOE4 = 1). The modules were then correlated to the group phenotype (e.g. all APOE3 Sham mice = 0, 0; all APOE3 TBI = 0, 1) using Pearson's correlation. Statistical significance was determined by student's *t*-test, $p < 0.05$. All modules were summarized by module eigengenes (ME), the first principle component of each module that was calculated as a synthetic gene representing the expression profile of all genes within a given module.

2.11. Western blot

Frozen cortices and hippocampi were homogenized in TBS homogenization buffer (250 mM sucrose, 20 mM Tris base, 1 mM EDTA, and 1 mM EGTA, 1 ml per 100 mg of tissue) and protease inhibitors cocktail (Roche) as described previously. For WB, RIPA extracted proteins were used for detection of apoE, ABCA1, CLU, FYN and β-ACTIN. Thirty microgram of proteins were resolved on 4–12% SDS-PAGE gels and transferred onto nitrocellulose membranes. Used were the following primary antibodies: Anti-ABCA1 (Ab7360, Abcam), anti-ApoE (178,479, Calbiochem), anti-FYN (sc-16, Santa Cruz), and anti-CLU (sc-6419, SantaCruz).

2.12. Statistical analyses

All results are reported as means ± S.E.M. To determine statistical significance between groups in EPM, we used two-way ANOVA with a Sidak's multiple comparison post hoc test. To analyze MWM data, a three-way ANOVA was used. Unless otherwise indicated, all statistical analyses were performed in GraphPad Prism, version 7.0, or R, version 3.3.2 and differences were considered significant where $p < 0.05$.

3. Results

3.1. TBI causes anxiety-related changes and spatial learning deficits

To examine the effect of APOE isoforms on cognitive performance following TBI, we used mice expressing human APOE3 or APOE4 isoform. As a model of brain injury, we used CCI, performed on 3 months old mice. First, the mice were tested for anxiety-related behavior in the elevated plus maze (EPM), 4 days post injury. As shown on Fig. 1A, the injured mice of both genotypes showed an increased time spent in the open-arms of the EPM when compared to their sham counterparts. We found significant main effects of genotype and TBI, but no interaction. Due to the acute time-point at which this test was performed, increased time spent in the open arms can be interpreted as an increased risk-taking or impulsive behavior by the injured animals.

We employed Morris Water Maze (MWM) to examine the effect of TBI on spatial learning. The result shown on Fig. 1B demonstrates that for both APOE genotypes, TBI significantly increased escape latency time in APOE3 mice (compare blue open and closed circles) and in APOE4 mice (compare red open and closed squares). As seen from Fig. 1B, APOE4 mice in both groups performed significantly worse than APOE3 mice confirming previous data from our and other groups showing a significant memory impairment at baseline in APOE4 mice (Fitz et al., 2012; Rodriguez et al., 2013; Fitz et al., 2013). The conclusion from these experiments is that TBI significantly worsens spatial learning and increases impulsive behavior in both APOE isoforms.

3.2. Changes in transcriptome induced by TBI reflect stimulated immune response and decreased neuronal functionality

To examine how TBI affects brain transcriptome, we performed mRNA-seq using total RNA isolated from the brains of the mice tested for cognitive performance and perfused 14 days post injury. For this analysis, we used hippocampal and cortical tissue from around the injury site. The PCA was used to calculate the principal components, which account for the sources of highest possible variance in the transcriptome. The result from the PCA shown on Fig. 2A demonstrates that the mRNA-seq data for TBI animals from both genotypes clustered together and the same was observed for sham treated mice. Thus, the result of the PCA suggests that the variance between gene expression levels in TBI vs Sham was higher than between gene expression level in APOE3 vs APOE4 transcripts.

An expression-by-expression plot (Y. Wang et al., 2015) using the lists of differentially expressed genes (Fig. 2B) demonstrates the high number of significantly expressed transcripts in all sham versus all TBI animals. We then compared the effect of TBI on transcriptome separately for each genotype. As shown on Fig. 2C and D, a significant number of differentially expressed genes was identified in both APOE groups (genes lists shown on Suppl. Table 1A and B). We were interested in whether there was a similarity between the biological processes affected by TBI in APOE3 and E4 mice. Top up-regulated categories in both genotypes were highly consistent and were associated with “Immune System Process”, “Innate Immune Response” and “Inflammatory Response” (Suppl. Table 2A and B). Top down-regulated categories in both genotypes were also similar, including “Regulation of Ion Transmembrane Transport”, and “Potassium Ion Transport” (Suppl. Table 3A and B). To further identify enriched pathways commonly affected by TBI in both isoforms, we applied Gene Set Enrichment Analysis (GSEA) (Subramanian et al., 2005) and compared all mice in the TBI group (E3-TBI + E4-TBI) to all sham mice (E3-sham + E4-sham). The analysis confirms the top up-regulated categories by TBI (Suppl. Fig. 1A).

We were particularly interested in two genes significantly up-regulated in brains of both APOE genotypes - *Abca1* transporter (fold change = 3.46) and Clusterin (*Clu/APOJ*, fold change = 1.66). As shown on Fig. 2E and F, the protein level of ABCA1 and CLU was significantly increased. In contrast, *Apoe* mRNA and APOE protein level were unaffected by TBI. Thus, these experiments confirm and validate our mRNA-seq results.

3.3. Transcriptome analysis demonstrates a higher expression of markers for resident microglia versus peripheral macrophages

Due to the nature of the CCI model, the blood brain barrier is damaged, which allows entry to peripheral cells not normally present in the brain, such as monocytes and peripheral macrophages. We were interested in identifying which cell type was responsible for the inflammatory response in the brain at 14 days post injury. To do this, we referred to Hickman et al. (2013), who demonstrated that microglia have a unique transcriptomic signature with several genes separate from that of peripheral macrophages. Thus, our RNA sequencing data point to a significant portion of genes that are considered microglia

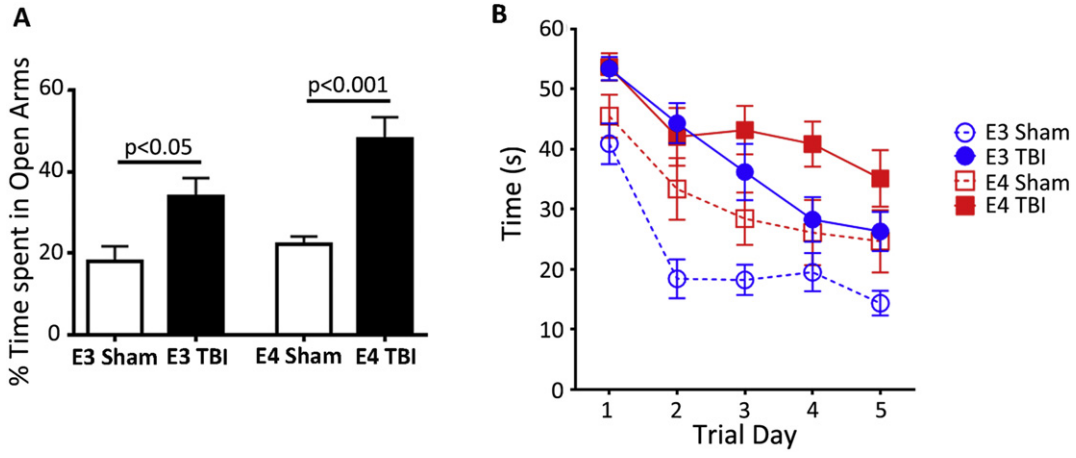

Fig. 1. TBI significantly affected behavior performance in mice expressing human APOE3 and APOE4 isoforms. Three months old APOE3 and APOE4 targeted replacement mice underwent CCI and their behavior performance was tested using Elevated Plus Maze (**A**) and Morris Water Maze (**B**) paradigms. (**A**) EPM was performed 4 days post injury. For both APOE isoforms, TBI significantly increased the time spent in the open arms of the maze compared to sham ($p < 0.0001$). Statistics is by two-way ANOVA. There is no interaction between genotype and injury but there are significant main effects of genotype ($F_{(1, 53)} = 4.967$, $p < 0.05$) and injury ($F_{(1, 53)} = 26.36$, $p < 0.0001$). Sidak's multiple comparison test showed a significant difference between APOE3-Sham vs APOE3-TBI ($p < 0.05$) and APOE4-Sham vs APOE4-TBI ($p < 0.001$). (**B**) Acquisition of spatial memory was examined in APOE3 (blue) and APOE4 mice (red) on 7–11 days post injury by MWM. Time to find the hidden platform is shown for all days of training. Statistics is by three-way ANOVA. There was no interaction between any of the factors, but significant main effects of all three, training, injury and genotype. (For training: $F_{(4, 4)} = 21.35$, $p < 0.0001$; for injury: $F_{(1, 4)} = 59.94$, $p < 0.0001$; for genotype: $F_{(1, 4)} = 17.8$, $p < 0.0001$).

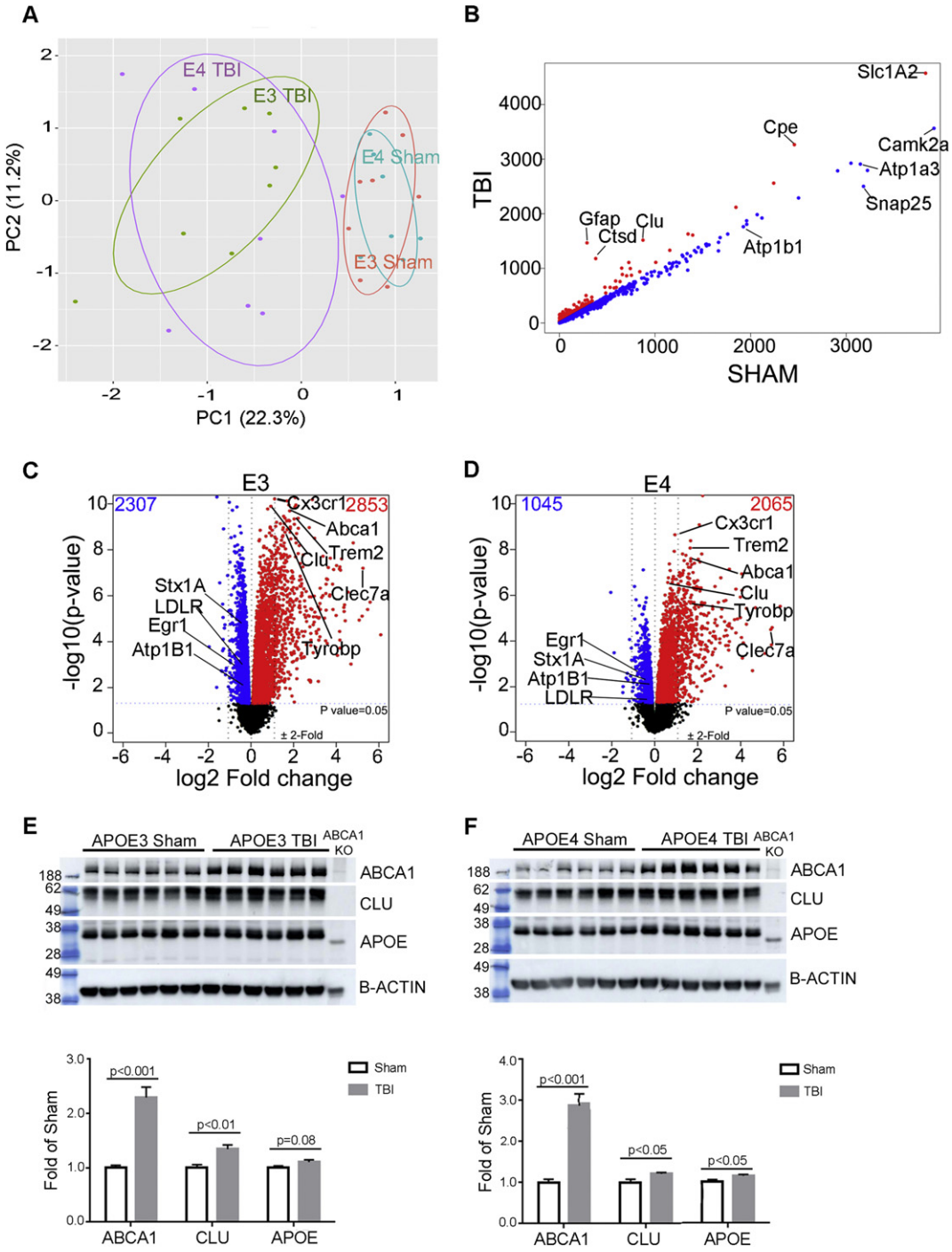

Fig. 2. TBI significantly affected the transcriptome demonstrating increases in immune response and decreases in neuronal functionality. mRNA-seq was performed on RNA isolated from the hippocampi and cortex of APOE3 and APOE4 mice shown on Fig. 1, $N = 8$ mice per group. (**A**) Principle component analysis used to calculate the principal components that account for the highest possible variance in the transcriptome. $N = 8$ mice/group and all transcripts from each mouse. PCA plot of the transcriptome shows distinct separation based on TBI but not on APOE isoform. (**B**) Scatterplot for genes comparing sham and TBI reads per million. (**C-D**) Volcano plots representing the mRNA-seq results. Differential gene expression analysis between sham and injured mice using EdgeR identified: in APOE3 (C): 2853 up- (red) and 2307 down-regulated genes by TBI (blue), and in APOE4 (D): 2065 up- and 1045 down-regulated genes at $p < 0.05$ cutoff. For C and D, statistics is by edgeR, $p < 0.05$. (**E**) Western blot results for APOE3 sham versus TBI animals for ABCA1, CLU, APOE, and β-ACTIN validate mRNA-seq results. (**F**) Western blot results for APOE4 sham versus TBI animals for ABCA1, CLU, APOE, and β-ACTIN validate mRNA-seq results. Proteins are normalized to levels of β-ACTIN.

"sensome" genes (86 of 100; Fig. 3A–B), or cellular receptors involved in the microglial function of sensing the brain environment. Several of those genes had a significantly higher expression in resident macrophages (microglia) when compared to peripheral macrophages, including *Gpr34*, *Trem2, Siglech*, and *P2ry12*. Additionally, a number of those genes are unique to microglia, including *Cx3cr1*, *Tmem119* and *Slco2b1*. We also looked at other receptor families involved in immune response, including the purinergic receptors (Fig. 3C–D) and sialic acid binding immunoglobulin lectins (*Siglecs*; Fig. 3E–F). Several of those were identified as being expressed at significantly higher levels in microglia compared to peripheral macrophages, including *P2rx7*, *P2ry6*, *P2ry12*, *P2ry13* and *Siglech*. As seen from Fig. 3A–F, all these groups of genes was significantly upregulated by TBI in both APOE3 and APOE4 mice. In contrast, several genes characteristic of peripheral macrophages,

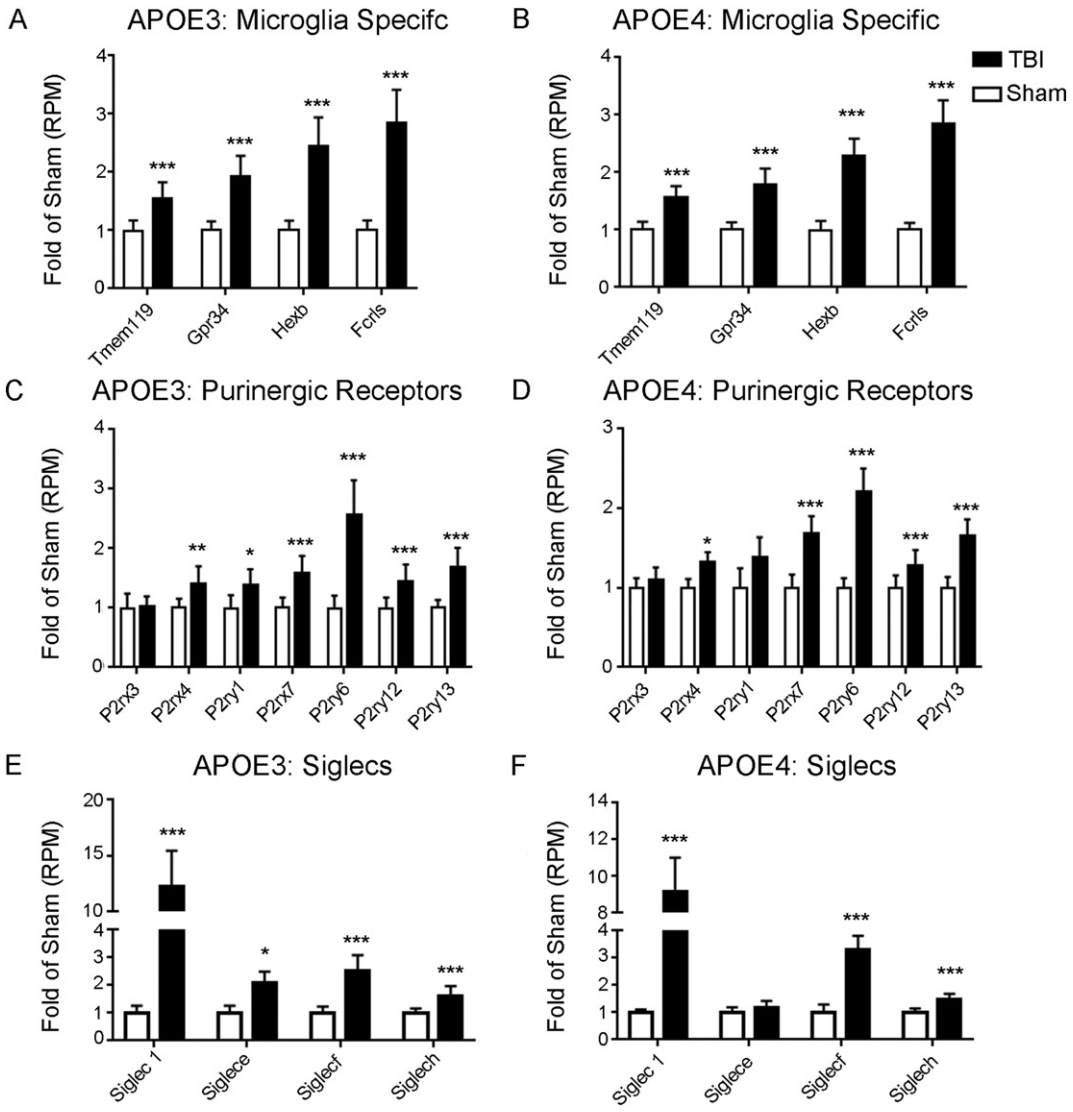

Fig. 3. mRNA-seq data reveal that microglia are predominant source of inflammation. Average expression according to mRNA-seq results for several inflammatory markers modulated by TBI were calculated as the fold of Sham reads per million for each gene. (**A**-**B**) Several microglial specific transcripts are significantly upregulated by TBI in both (A) APOE3 and (B) APOE4 mice. (**C**-**D**) Purinergic receptors in (C) APOE3 and (D) APOE4 mice, as well as (**E**-**F**) Siglecs in (E) APOE3 and (F) APOE4 mice were also upregulated following TBI. Statistics is by edgeR; $^{*}p < 0.05$, $^{**}p < 0.01$, $^{***}p < 0.001$.

such as *Alox15*, *Fabp4*, *Fcna*, *Slp1 and Serpinb2* were not found (data not shown) or expressed at a very low level (*P2rx4*). We conclude that whereas the peripheral macrophages invade in the initial days following TBI and are likely to remain present in CNS at low levels, the resident microglia are the predominant source of inflammatory response in the brain 14 days post injury (Gyoneva and Ransohoff, 2015; Holmin et al., 1995; Kelley et al., 2007).

3.4. Integrated system approach identifies correlated gene networks associated with TBI

To identify gene networks affected by TBI, we employed Weighted Gene Co-expression Network Analysis (WGCNA) (Zhang and Horvath, 2005; Richter et al., 2014). We used datasets of the same APOE3 and APOE4 expressing mice, shown on Figs. 2 and 3. WGCNA clusters genes based on expression profiles into functional groups (referred to as modules) and the average expression profile is represented as a 'module eigengene' (ME), which is given an arbitrary colour name. MEs were then correlated to the phenotype of each experimental group, namely APOE3-TBI, APOE4-TBI, APOE3-Sham and APOE4-Sham, allowing identification of the networks associated with them. We found no significant gender difference, therefore male and female mice were analyzed together. The relationship table (Fig. 4) shows the Pearson correlation of each module to the phenotype. Additionally, the table visualizes the overall direction of expression for the genes within each module for each phenotype. We were most interested in modules that correlated significantly with either injury in both APOE isoforms or with APOE isoform. Thus, we chose to further characterize two networks that correlate to TBI (ME Brown and ME Green), and two to APOE genotype (ME Darkred and ME Salmon). Correlations between the modules are shown in Suppl. Fig. 2.

ME Brown positively correlated to APOE3-TBI ($r = 0.54$, $p = 0.002$) and APOE4-TBI groups ($r = 0.47$, $p = 0.007$) and negatively correlated to sham treated mice. The interpretation of the positive correlation is that TBI increases the expression of genes, members of this module in mice expressing either isoform. This network is enriched with transcripts functionally associated with "Immune Response" and "Innate Immunity" (Table 1). As seen in Suppl. Fig. 3C and D, the correlation between Module membership and Gene significance for genes within this network demonstrates that they strongly relate to the biological

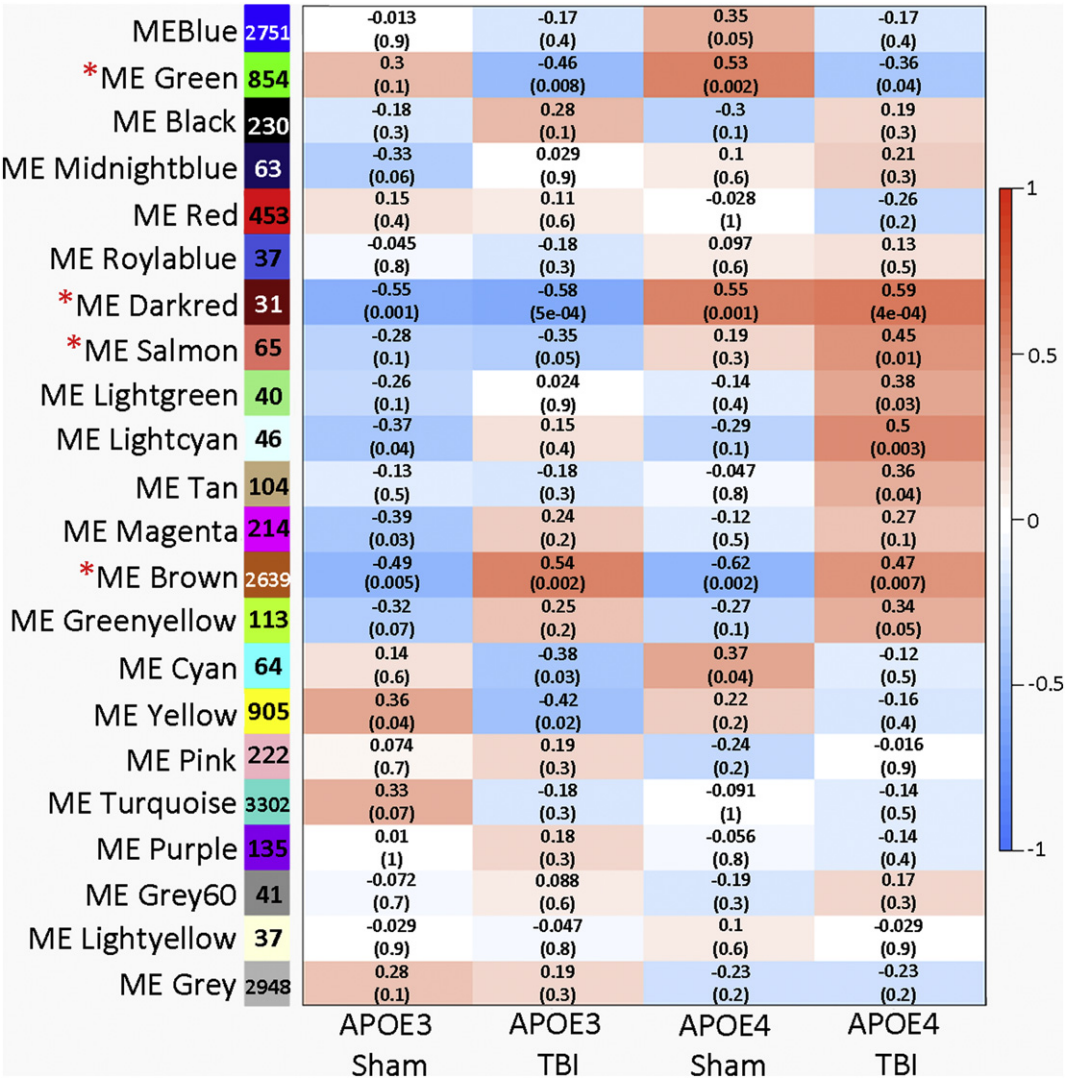

Fig. 4. WGCNA identified modules that correlated to TBI and or APOE isoform. WGCNA was used to determine the correlation of module eigengenes to Injury and APOE genotype. Each cell shows the correlation between the module eigengene (rows) and group (columns) with *P*-value. Red denotes a positive and blue is a negative correlation. Modules of interest are differentially expressed between trait conditions. Brown, and green are modules associated with TBI, Darkred and Salmon – with APOE genotype.

Table 1
Gene-network modules represent various biological functions associated with injury and APOE isoform. Networks of interest include ME Brown and ME Green, which are associated with injury, and ME Darkred and ME Salmon, which are associated with APOE isoform. Shown are the top GO terms for each module; bold denotes representative GO term(s) assigned to the module.

Module name	Effect	*P*-value	Gene count	GO terms	Enrichment *P*-value
Brown	Injury	1.0E-10	2639	**Immune response**	9.97E-41
				Innate immune response	1.16E-28
				Phagocytosis	2.61E-05
Green	Injury	5.0E-06	854	**Transport**	1.98E-04
				Phospholipid transport	0.0016
Darkred	Genotype	1.0E-23	31	**Innate immune response**	0.0428
				Complement Activation	0.0471
Salmon	Genotype	0.001	65	**Myelination**	3.73E-05
				Oligodendrocyte differentiation	1.06E-04

processes associated with this module. The expression levels for all genes in the network and for each sample are shown on Fig. 5A (heatmap and bar plot). The network (Fig. 5B) was built using hub genes associated with immune response and phagocytosis, such as *Trem2* (Triggering Receptor Expressed on Myeloid Cells 2), *Tyrobp*, *Clec7a*, *Cd68*, *Cx3cr1* and the transcripts connected to them. Hub genes of this network are highly enriched in microglia signature genes (fold enrichment 8.95), including *Grp34*, *Fcrls*, *Tmem119* and *Cx3cr1*. In the hub gene list, there were also astrocyte-specific genes, such as *Gfap*, *Aqp4*, *Clu* (fold enrichment 8.69).

To validate the mRNA-seq results shown on Fig. 5C and D, we performed RT-QPCR for several genes - *Trem2*, *Tyrobp*, *Cx3cr1*, *Tgfb1*, *Tgfbr1* (Fig. 5E and F). To confirm that mRNA expression levels correspond to an increase in the levels of the respective proteins, we chose three genes highly affected by TBI – *Trem2* and *Aif1*/*Iba-1* expressed in microglia and *Gfap* expressed in astrocytes. *Trem2* encodes a transmembrane protein that is expressed on myeloid lineage cells, including microglia and recent studies have shown that *Trem2* variants affect microglial functionality (Colonna and Wang, 2016). To analyze the impact of TBI on the protein level of TREM2, AIF1/IBA-1 and GFAP, we performed immunohistochemistry on brain sections from the same mice.

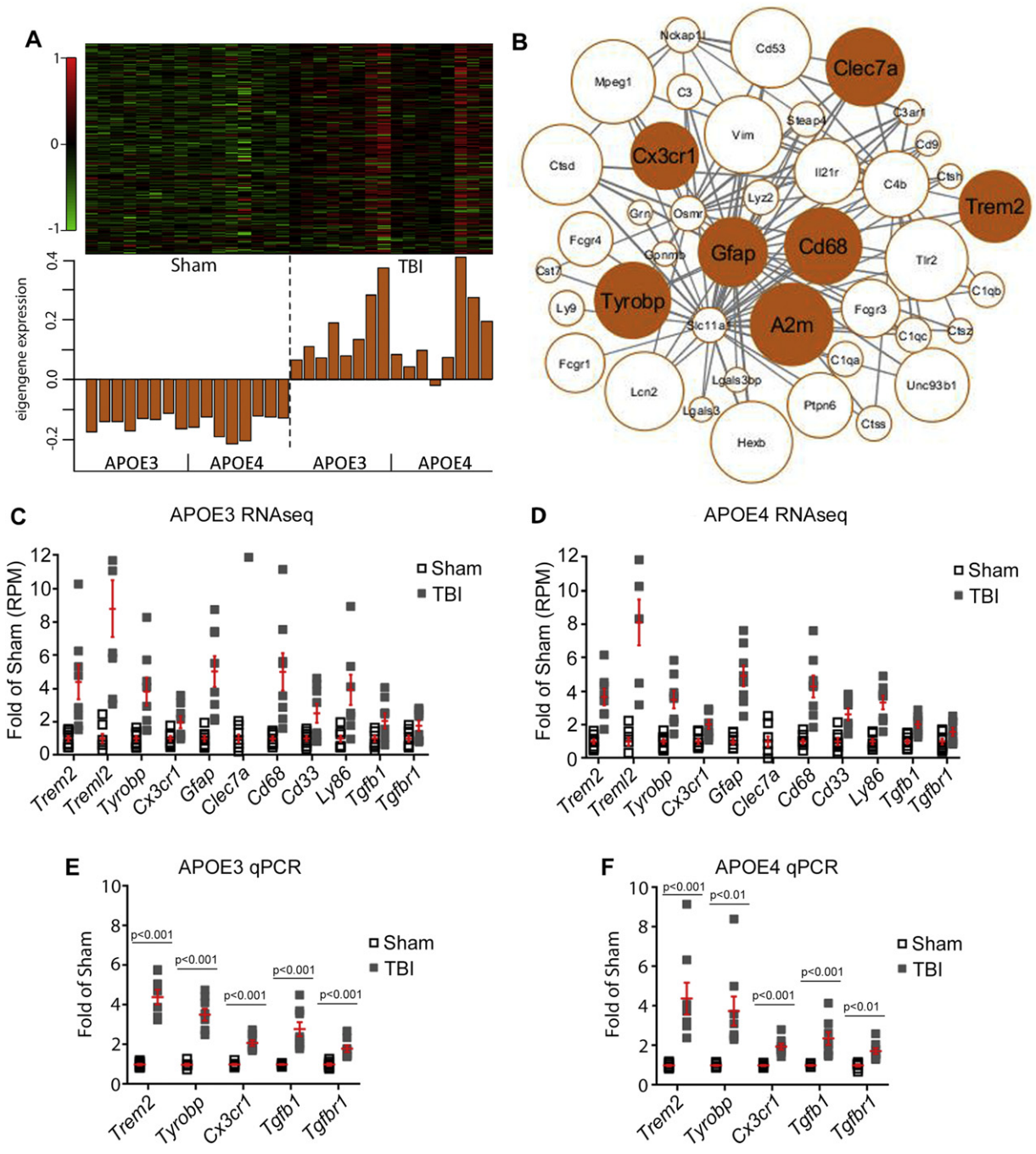

Fig. 5. ME Brown correlates to TBI and is associated with Immune Response. (**A**) Expression barplot shows the gene expression and eigengene expression within each sample. Within the heatmap, the rows denote genes and the columns correspond to samples, with the corresponding module eigengene value for each sample shown in the bar plot below. Red denotes over-expression and green under-expression of the gene within the sample. (**B**) Network of genes connected to hub genes *Trem2*, *Tyrobp*, *Clec7a*, *Cd68*, *Cx3cr1* representing immune response. Size of each gene was determined by modular membership value, and the weight determined edge width. (**C-D**) Average expression according to mRNA-seq results of genes modulated by TBI in "Immune response" category for (C) APOE3 and (D) APOE4 mice. The average expression was calculated as fold of Sham reads per million for each gene. Statistics is by edgeR, $p < 0.05$. (**E-F**) Validation of mRNA-seq results for *Trem2*, *Tyrobp*, *Cx3cr1*, *Tgfb1*, *Tgfbr1* for (E) APOE3 and (F) APOE4 mice by qPCR. Statistics was determined by *t*-test.

As seen in Fig. 6A, sham animals showed relatively low-to-no TREM2 immunostaining. In contrast, TBI significantly increased presence of TREM2 around the injury site in both APOE3 (Fig. 6B) and APOE4 (Fig. 6C) mice ($p < 0.05$). IBA1 staining shown on Suppl. Fig. 4 is consistent with the increased intensity of TREM2 around the injury site and confirms microglia activation after TBI. For both TREM2 and IBA-1 staining, there was no significant difference between APOE3 and APOE4 injured animals. To validate the increased mRNA expression of GFAP, we performed immunohistochemistry against GFAP. As visible from Fig. 6E, sham animals show evenly distributed low levels of GFAP staining. In contrast, TBI animals show significantly higher levels of GFAP staining in both APOE3 and APOE4 when compared to their sham counterparts (Fig. 6F-G). As with TREM2 and IBA-1, there was no significant APOE isoform dependent difference in GFAP staining of either sham or TBI groups. The high levels of astrocytosis and microgliosis present at the injury site demonstrate a recruitment of these cells types to the injury.

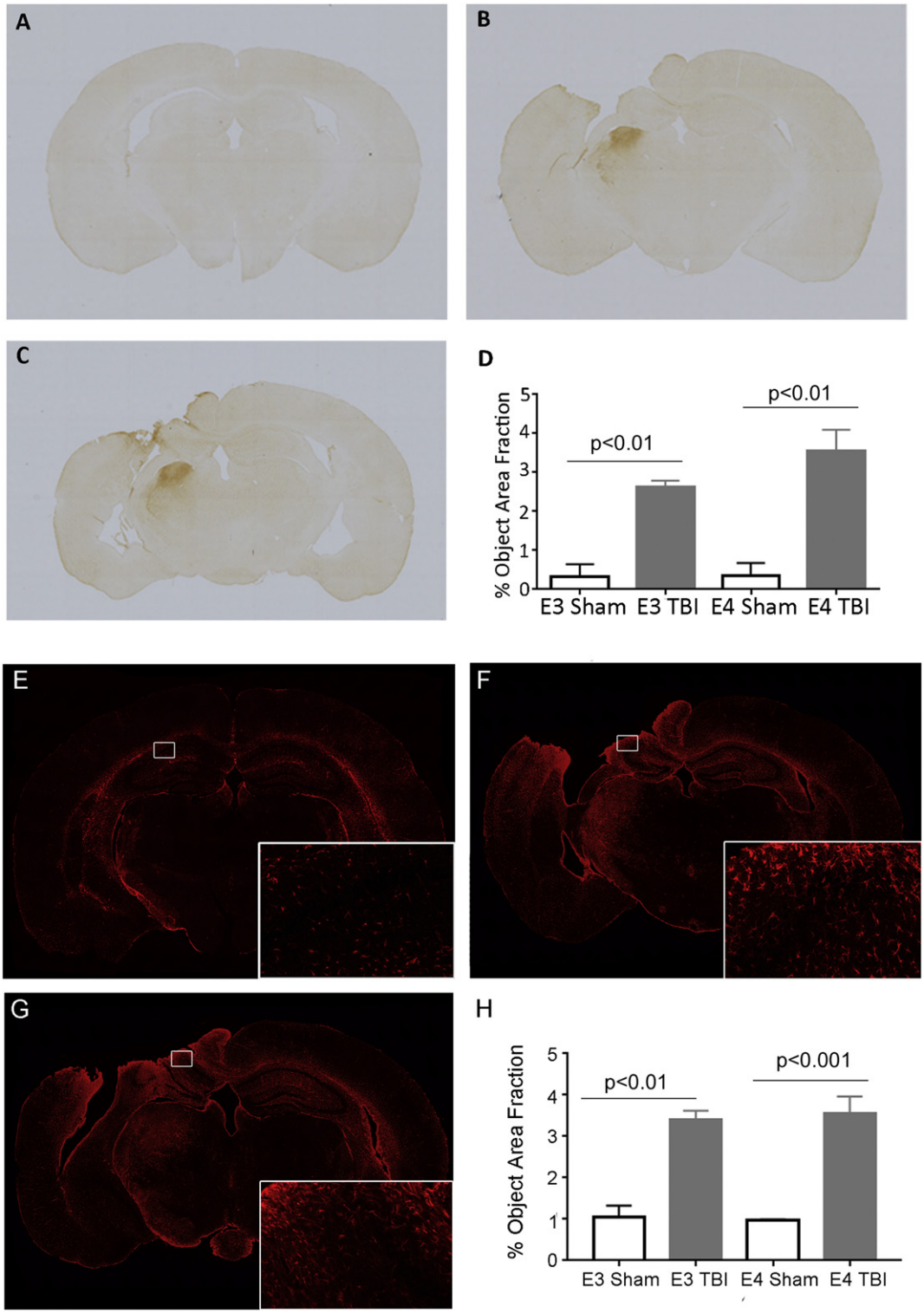

Fig. 6. TREM2 protein level and Astrocytosis are increased by TBI. Immunohistochemistry with anti-TREM2 antibody or anti-GFAP was performed in both sham and TBI mice ($n = 3$/group). Percent intensity of Trem2 staining or GFAP staining was determined in the ipsilateral hemispheres. (**A**) Sham animals had low to no levels in Trem2. (**B**) APOE3 TBI and (**C**) APOE4 TBI animals had significantly higher levels of Trem2 when compared to their sham counterparts ($p < 0.01$ for both APOE3 and APOE4). (**D**) Analysis of object area fraction demonstrates a significant main effect of injury ($p < 0.001$), but not APOE isoform in Trem2 levels. Statistics is by Two-way ANOVA with post-hoc Tukey's multiple comparisons test. (**E**) Sham animals demonstrated low GFAP staining levels. (**F**) APOE3 and (**G**) APOE4 TBI animals show increased GFAP staining compared to their sham counterparts, particularly near the injury site (APOE3: $p < 0.01$; APOE4: $p < 0.001$). Insets taken from the injury visualize the increased staining at higher magnification (20×). (**H**) Analysis of object area fraction demonstrates a significant main effect of injury ($p < 0.001$), but not APOE isoform in GFAP levels. There was no significant difference between APOE3 and APOE4 animals, regardless of injury. Statistics is by Two-way ANOVA with post-hoc Tukey's multiple comparisons test.

The conclusion from these data is that, in both APOE isoforms, TBI affects resident microglia genes functionally related to immune response and phagocytosis, as well as astrocyte specific genes.

ME Green is negatively associated with injury suggesting that genes, members of this module are downregulated by TBI (Suppl. Fig. 5). The related biological process that represents this network (module size

= 854) was associated with GO category "Transport" and is represented by *Camk2b, Pik3r2* and *Pld3* for which genetic variants are associated with an increased risk of Alzheimer's disease (Hooli et al., 2015; C. Wang et al., 2015) and functionally have a role in hippocampal plasticity, phospholipid metabolism, brain development, and APP processing (Cruchaga et al., 2014).

3.5. Networks associated with expressed APOE isoform

As shown on Fig. 4, ME Darkred (Fig. 7, Suppl. Fig. 6) and Salmon (Fig. 8, Suppl. Fig. 6) are significantly associated with APOE isoform regardless of injury. On Fig. 7A, the heat-map and bar plot representing ME Darkred demonstrate an increased expression of genes associated with this network in APOE4 mice (TBI + Sham) and a decreased expression in APOE3 mice (TBI + Sham). The biological process associated with ME Darkred network (module size = 31) was the GO term "Innate immunity" (Fig. 7B). The heatmap (Fig. 7C) shows the highest 50 upregulated genes when comparing APOE3 and APOE4 mice. We were interested and further validated one of the hub genes associated with BP "Innate Immunity" - *Fyn* (Fyn proto-oncogene, Src family tyrosine kinase). *Fyn* is a major regulator of pro-inflammatory processes, specifically microglia mediated neuroinflammation (Panicker et al., 2015). mRNA-seq (Fig. 7D) and protein expression level for *Fyn* are shown on Fig. 7E and F. Three of *Serpina3* genes (*Serpina3m*, *Serpina3f and Serpina3h*) have been also identified as hub genes in this network.

ME Salmon positively correlated to APOE4-TBI mice and negatively to APOE3-TBI ($r = 0.41$, $p = 0.01$). Functionally, this module (module size = 65) is enriched in genes connected to the BP "Myelination"

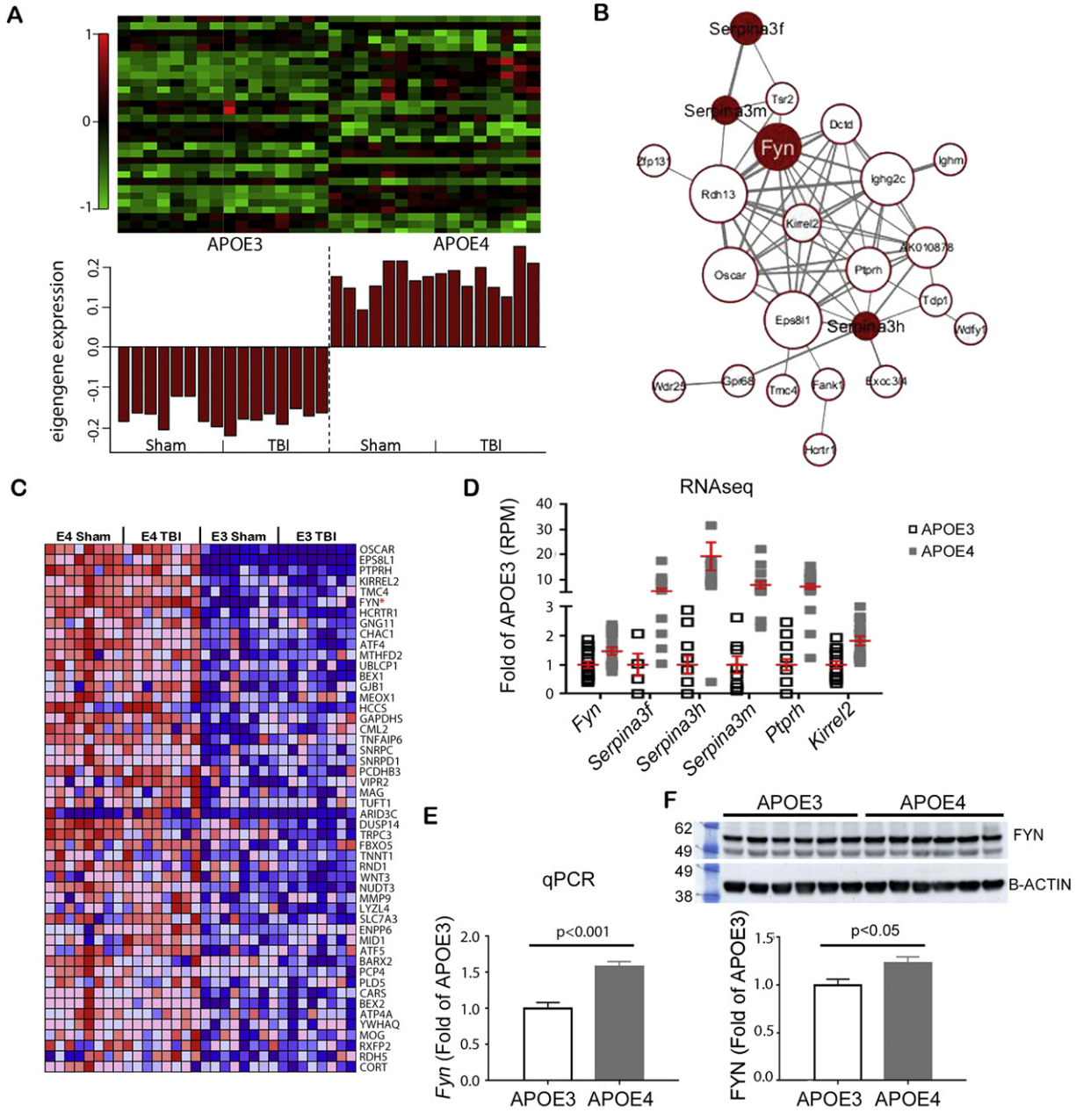

Fig. 7. ME darkred correlates to APOE isoform and is associated with innate immunity. (**A**) The expression bar plot shows the gene expression and eigengene expression within each sample. (**B**) Network of genes connected to the chosen hub gene *Fyn* representing innate immunity. (**C**) Heatmap of top 50 upregulated genes in comparing APOE3 to APOE4 mice. (**D**) mRNA-seq results for important genes within the network. The average expression was calculated as fold of APOE3 reads per million for each gene. Statistics is by edgeR, $p < 0.05$. (**E**) Validation of mRNA-seq results by qPCR. Statistics was determined by *t*-test. (**F**) Western blot results for APOE3 TBI versus APOE4 TBI animals for FYN and β-ACTIN validate mRNA-seq results. Proteins are normalized to levels of β-ACTIN and presented as fold of APOE3.

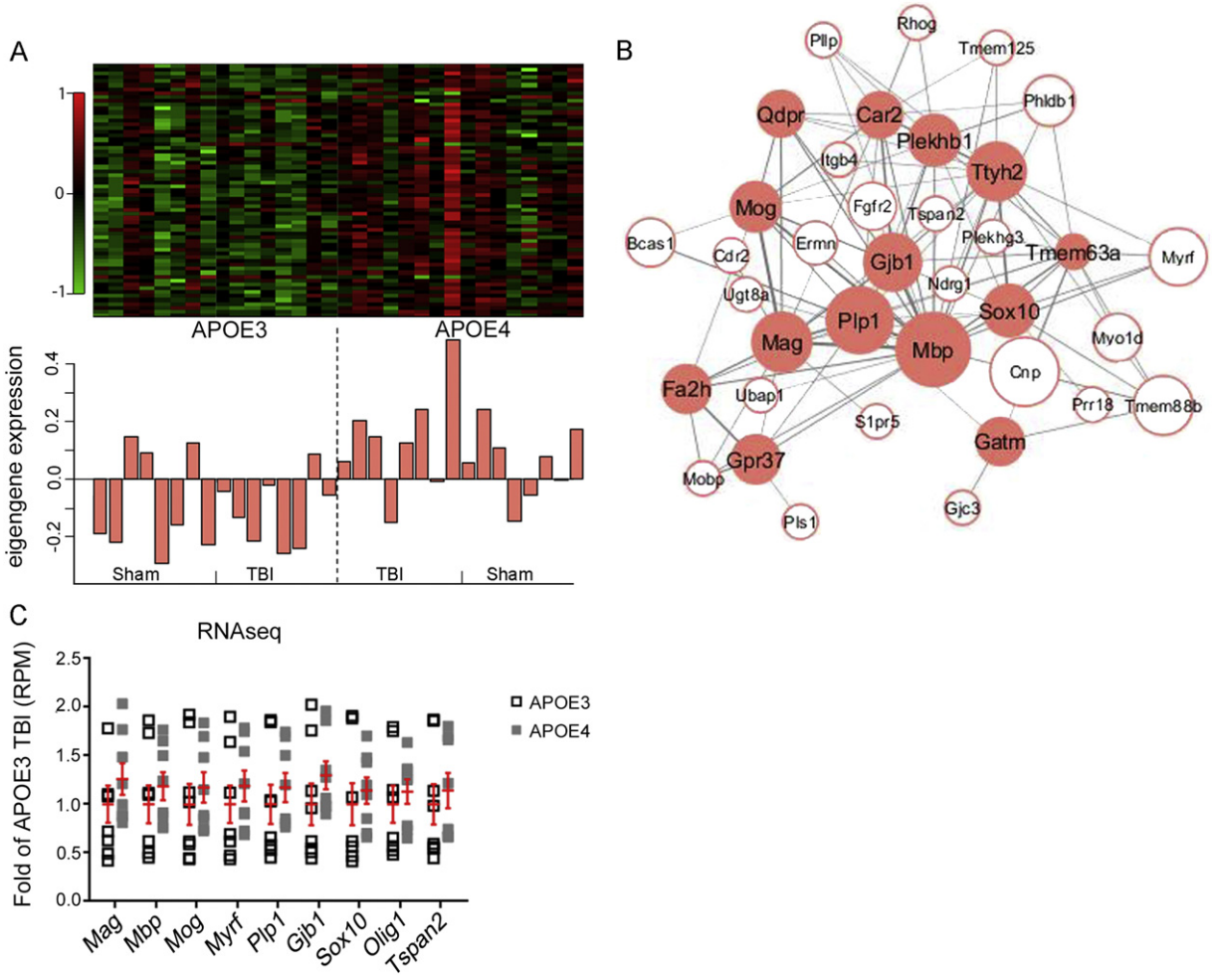

Fig. 8. Gene-network module salmon correlates to APOE isoform in injury groups and is associated with myelination. (**A**) The expression barplot shows the gene expression and eigengene expression within each sample. (**B**) Network of genes connected to hub genes *Car2*, *F2ah*, *Mbp* and *Plp1* representing myelination. (**C**) mRNA-seq results for important genes within the network. The average expression was calculated as fold of APOE3 TBI reads per million for each gene. Statistics is by edgeR, $p < 0.05$. (**D**) Validation of mRNA-seq results by qPCR for *Mbp* and *Plp1*. The average expression was calculated as fold of all APOE3 TBI mice. Statistics was determined by *t*-test.

(Fig. 8 and Table 1). The network is significantly enriched with oligodendrocyte signature genes (18 genes out of 64 were oligodendrocyte specific). The representative network (Fig. 8B) was built using the hub genes *Car2*, *F2ah*, *Mbp* and *Plp1* that are all coding for major components of myelin (Alderson et al., 2006; Bujalka et al., 2013) and together with cholesterol, are particularly important for myelin formation and remodeling in the context of axonal loss and repair after TBI (Saher et al., 2005; Saher and Stumpf, 2015). Mutations in the majority of the genes within the network lead to demyelination and hypomyelinating inherited disorders (Chrast et al., 2011; Saher and Stumpf, 2015; Schiza et al., 2015; Tsai et al., 2016), or have been implicated in neurodegeneration, including Alzheimer's Disease. Alternatively, the high presence of myelin related proteins, including *Mag*, myelin associated glycoprotein, could be indicative of the formation of a glial scar (Yiu and He, 2006; Rolls et al., 2009). Chronically, a glial scar could prevent axonal regeneration and potentially explain a worse outcome in APOE4 TBI mice. mRNA-seq results between APOE4 TBI and APOE3 TBI for selected hub genes are shown on Fig. 8C.

4. Discussion

We examined the role of human APOE isoforms in the response to TBI in mice. Our study was designed with the goal to identify differences in cognitive performance, brain transcriptome and genome-wide correlated gene networks in adult (3-month-old) APOE targeted replacement mice, following CCI model of brain injury. We found that TBI significantly worsened performance in the anxiety-related EPM and the spatial learning task MWM, but the results showed no interaction of injury with APOE isoform. At baseline, animals expressing APOE4 had pre-existing deficits compared to APOE3 animals, but both groups displayed similar responses to injury although in general APOE3 mice performed better. In mice expressing either isoform, TBI significantly changed the transcriptome, particularly increasing the expression of genes related to immune response and phagocytosis, such as *Trem2*, *Tyrobp*, *Clec7a*, *Cd68*, *Cx3cr1*, with low to no expression of peripheral macrophage genes, such as *Alox15* and *P2rx4*. We analyzed the effect of TBI on the transcriptome within each genotype and found similar biological processes affected, regardless of the genotype. The GO terms downregulated by TBI were also similar, with the top processes being regulation of transmembrane ion transport and potassium transport. We did identify an APOE isoform effect on the brain transcriptome in TBI mice, but this effect was entirely separate from the effect of injury.

Using WGCNA we identified correlated gene networks associated with TBI. We determined differential effects of two traits – genotype and type of injury, and identified gene networks throughout the entire genome, that correlated with injury and with the expressed APOE isoform. To a very significant extent, WGCNA results confirmed the GO terms identified through pathway analysis using the lists of differentially expressed genes in response to TBI. Most highly affected by TBI

network was represented by "Immune Response". Importantly, neither APOE3 or APOE4 isoform had a specific modulatory effect on this network: validations of several genes by RT-qPCR, including *Trem2* by IHC, found no differences between mice expressing APOE3 or APOE4 (Figs. 5 & 6). This network was highly enriched in microglia signature genes; among those, *Trem2*, *Clex7a* and *Hexb* were identified as hub genes suggesting that at our chosen time-point – 14 days post injury, the elevated immune response in the brain was predominantly a result of activated microglia and astrocytes, which was confirmed by immunohistochemistry and is consistent with TREM2 localization. Recently, human TREM2 has come under scrutiny for its role in inflammation and neurodegeneration. *TREM2* is expressed solely in cells of myeloid lineage, including microglia, and *TREM2* mutations or mutations in the gene *TYROBP*, coding for its adaptor protein (aka *DAP12*) are linked to Nasu-Hakola disease (Bianchin et al., 2004). Although its natural ligands are unknown, binding of TREM2 to negatively charged lipids, results in TYROBP phosphorylation, activation of intracellular spleen tyrosine kinase SYK, and thus SYK-RAS-ERK signaling pathway, actin remodeling and calcium mobilization needed for phagocytosis (Colonna and Wang, 2016). Using fluid percussion model of injury in *Trem2* deficient mice Lamb's group has recently shown that in injured mice there was a reduction of infiltrating macrophages, reduced inflammatory cytokines, less hippocampal volume loss and a rescue of spatial memory deficits (Saber et al., 2016). Yet, a different study found that *Trem2*$^{-/-}$ mice had decreased phagocytosis after stroke and worsened neurological outcomes (Kawabori et al., 2015). Obviously, the contradictory results of these studies point to the need of standardized study designs and data collection to understand the role of TREM2 in the response to TBI and subsequent repair.

The "Transport" network, ME Green, was significantly affected and down-regulated by injury in both genotypes. The hub genes of this network include *Camk2b*, which is important for both hippocampal-dependent learning and long-term potentiation (Borgesius et al., 2011). The kinase transcribed by *Camk2b* is necessary for the proper targeting of CAMK2a at the synapse for promotion of dendritic spines and synapse formation. *Pld3* is another gene in the "Transport" network, which is highly expressed in the brain and may be involved in synaptic transmission and signal transduction (Cruchaga et al., 2014). A rare missense variant of *PLD3* was linked to an increased risk of late onset AD and since a decreased expression of PLD3 is associated with higher levels of extracellular Aβ, PLD3 may have some role in APP processing (Osisami et al., 2012).

In injured mice "Innate immunity" was the network of genes differentially affected by APOE isoform. The network was built of transcripts connected to *Fyn* and *Serpina3*. Since tau and *Fyn* have been shown to co-localize in dendrites, not surprisingly, recent studies have suggested a pathogenic role for *Fyn* in AD, (Lau et al., 2016). FYN interacts with Aβ, which possibly serves as a critical step in triggering downstream neuronal pathology. Moreover, it has been suggested that binding of Aβ oligomer species to the neuronal membrane receptors at the post-synaptic terminal may activate FYN by phosphorylation, resulting in *N*-methyl-D-aspartate (NMDA) receptor phosphorylation, dendritic spine loss and tau phosphorylation (Nygaard et al., 2014). *Serpina3m*, *Serpina3f and Serpina3h - Serpina3* genes identified as hub genes in ME Darkred, reside on mouse chromosome 12 (*12F1* locus) and code for isoforms of the plasma protease inhibitor α1-antichymotrypsin (Forsyth et al., 2003). Initially, SERPINA3 binding to Aβ peptide and subsequent deposition of this complex in amyloid plaque has been linked to the progression of Alzheimer's disease (see (Abraham, 2001) for review). Genetic variants of α1-antichymotrypsin have been considered as increasing the risk of LOAD, or a modifier of the risk imposed by *APOE4* (Guan et al., 2012; Kamboh et al., 1995). Results of more recent studies, however, have demonstrated a neuroprotective effect of the protein SERPINA3 in in vitro and in vivo models of multiple sclerosis, as well as accelerated tissue repair in a diabetic mouse model (Hsu et al., 2014; Haile et al., 2015).

The "myelination" network represented by ME salmon was differentially affected by APOE isoform within only the injury groups. ME Salmon was upregulated in APOE4 TBI mice and downregulated in APOE3 TBI mice, and not significant in sham groups. The network was built on several myelin related proteins, such as *Car2*, *F2ah*, *Mbp* and *Plp1*, and was also highly enriched in oligodendrocyte specific markers. The presence of oligodendrocytes after injury is not surprising, as myelin and cholesterol would both be necessary components for axonal repair and regeneration (Saher et al., 2005; Saher and Stumpf, 2015). However, myelin related proteins, particularly *Mag*, which was identified as a hub gene within the network, have been associated with inhibited axonal outgrowth and the formation of a glial scar (Yiu and He, 2006). The role of this network in repair and scar formation could provide a mechanism for worse outcome in APOE4 isoform after TBI that is temporally dependent.

The underlying molecular mechanisms by which human APOE isoforms, globally expressed in a mouse, affect the outcome of TBI are not clear, and in general are poorly understood. While controversial in their findings and final interpretation, many studies have suggested, so far, that the inheritance of *APOE4* allele in humans or the expression of APOE4 in animal models would result in a worse outcome following brain injury. Several human studies, however, have shown that APOE4 had no effect on outcome of TBI (Chamelian et al., 2004; Moran et al., 2009). In contrast, the majority of animal studies, mostly in AD mouse models expressing human APP, have demonstrated APOE4 plays a significant role in determining the pathology and recovery following TBI, possibly in an age dependent manner (Bennett et al., 2013; Mannix et al., 2011; Bird et al., 2016). The animal models of TBI obviously do not, and cannot, represent all aspects of brain pathology as a response to brain trauma at molecular, cellular and organ levels. Moreover the lack of standardized study design and data collection makes it extraordinarily difficult to compare the results of the studies performed so far and to draw definitive conclusions. The results of our study did not suggest a major role for APOE3 or APOE4 isoforms in modulating the response to TBI. We identified, however, networks of genes in brains of APOE3 and APOE4 injured mice that have clearly pointed out to genes, and thus their proteins, with a potential to become useful and rational targets for future research and drug discovery relevant to TBI.

The major physiological role of APOE, as a principal apolipoprotein of HDL-like particles in brain, is to transport cholesterol and phospholipids in brain interstitial space/fluid. Thus, it is reasonable to assume that other genes/proteins, involved in brain cholesterol metabolism with a regulatory role in *APOE* expression or in the brain cell type specific transport of cholesterol may play an equally significant, if not a larger role in the response to injury. In our sequencing datasets and validation assays we found that following injury *Abca1* mRNA and ABCA1 protein levels were increased. An increased ABCA1 protein level in a rat model of TBI has already been reported (Cartagena et al., 2008). Thus, the elevated expression of ABCA1 following TBI could be a response to the increased demand for cholesterol and phospholipids, necessary for axonal repair. The hub genes in ME Salmon provide additional support that a correlated response to TBI includes upregulation of network of genes relevant to cholesterol transport and myelin formation. While in normal conditions in adult, developed brain oligodendrocytes synthesize cholesterol and do not depend on cholesterol transported by APOE particles, they express LDL-R and receptor mediated endocytosis of lipoproteins, APOE included, is a very important transport mechanism for cholesterol supply in traumatized brain areas with axonal damage and undergoing myelination/myelin remodeling. APOE mediated stimulation of Neural Stem Cells and enhanced oligodendrogenesis, which require sufficient amounts of cholesterol and phospholipids, and to some extent APOE/LDL-R interaction for activation of downstream signaling cascades, most probably have an important role for improved myelination and axonal restoration as part of the recovery process.

In conclusion, we found that APOE3 and APOE4 targeted replacement mice demonstrate similar cognitive impairment following

moderate TBI with differences reflecting the preexisting deficits in APOE4 mice at baseline. Transcriptional profiling 14 days following TBI revealed a clear separation between sham and injured animals without a difference based on APOE isoform. Top up-regulated categories in both genotypes were highly consistent and were associated with Immune System, Innate Immune and Inflammatory Responses. Ion and Potassium Transport categories were downregulated, similarly in both genotypes. Using WGCNA, we determined that TBI and APOE affected separate networks independently. Immune Response was the most affected network driven by TBI in both genotypes, while both sham and injured animals were differentially affected by APOE isoform, with increased expression of genes associated with functional groups/modules representing Innate Immunity. The network representing Myelination was affected by APOE isoform across the injury groups, demonstrating a difference in response to injury between APOE3 and APOE4 mice. The results of this study indicate that distinct cellular pathways/networks drive the APOE isoform specific phenotype and the response to TBI at this acute time point.

Conflict of interest

The authors declare that they have no conflict of interest.

Acknowledgements

Supported by National Institutes of Health (R01AG037481, R01AG037919, K01AG044490, R01ES024233) and U.S. Department of Defense (W81XWH-13-1-0384). We would like to thank Dr. H. I. Kamboh for technical assistance.

Appendix A. Supplementary data

Supplementary data to this article can be found online at http://dx.doi.org/10.1016/j.nbd.2017.05.006.

References

Abraham, C.R., 2001. Reactive astrocytes and alpha1-antichymotrypsin in Alzheimer's disease. Neurobiol. Aging 22, 931–936.

Acosta, S.A., Tajiri, N., Shinozuka, K., Ishikawa, H., Grimmig, B., Diamond, D.M., Diamond, D., Sanberg, P.R., Bickford, P.C., Kaneko, Y., Borlongan, C.V., 2013. Long-term upregulation of inflammation and suppression of cell proliferation in the brain of adult rats exposed to traumatic brain injury using the controlled cortical impact model. PLoS One 8, e53376.

Alderson, N.L., Maldonado, E.N., Kern, M.J., Bhat, N.R., Hama, H., 2006. FA2H-dependent fatty acid 2-hydroxylation in postnatal mouse brain. J. Lipid Res. 47:2772–2780. http://dx.doi.org/10.1194/jlr.M600362-JLR200.

Alexander, S., Kerr, M.E., Kim, Y., Kamboh, M.I., 2007. Apolipoprotein E4 allele presence and functional outcome after severe traumatic brain injury. J. Neurotrauma 24, 790–797.

Bennett, R.E., Esparza, T.J., Lewis, H.A., Kim, E., Mac Donald, C.L., Sullivan, P.M., Brody, D.L., 2013. Human apolipoprotein E4 worsens acute axonal pathology but not amyloid-beta immunoreactivity after traumatic brain injury in 3xTG-AD mice. J. Neuropathol. Exp. Neurol. 72:396–403. http://dx.doi.org/10.1097/NEN.0b013e31828e24ab.

Bianchin, M.M., Capella, H.M., Chaves, D.L., Steindel, M., Grisard, E.C., Ganev, G.G., da Silva Junior, J.P., Neto Evaldo, S., Poffo, M.A., Walz, R., Carlotti Junior, C.G., Sakamoto, A.C., 2004. Nasu-Hakola disease (polycystic lipomembranous osteodysplasia with sclerosing leukoencephalopathy—PLOSL): a dementia associated with bone cystic lesions. From clinical to genetic and molecular aspects. Cell. Mol. Neurobiol. 24, 1–24.

Bird, S.M., Sohrabi, H.R., Sutton, T.A., Weinborn, M., Rainey-Smith, S.R., Brown, B., Patterson, L., Taddei, K., Gupta, V., Carruthers, M., Lenzo, N., Knuckey, N., Bucks, R.S., Verdile, G., Martins, R.N., 2016. Cerebral amyloid-beta accumulation and deposition following traumatic brain injury—a narrative review and meta-analysis of animal studies. Neurosci. Biobehav. Rev. 64:215–228. http://dx.doi.org/10.1016/j.neubiorev.2016.01.004.

Borgesius, N.Z., van Woerden, G.M., Buitendijk, G.H., Keijzer, N., Jaarsma, D., Hoogenraad, C.C., Elgersma, Y., 2011. betaCaMKII plays a nonenzymatic role in hippocampal synaptic plasticity and learning by targeting alphaCaMKII to synapses. J. Neurosci. 31: 10141–10148. http://dx.doi.org/10.1523/JNEUROSCI.5105-10.2011.

Brody, D.L., Mac Donald, C., Kessens, C.C., Yuede, C., Parsadanian, M., Spinner, M., Kim, E., Schwetye, K.E., Holtzman, D.M., Bayly, P.V., 2007. Electromagnetic controlled cortical impact device for precise, graded experimental traumatic brain injury. J. Neurotrauma 24:657–673. http://dx.doi.org/10.1089/neu.2006.0011.

Bujalka, H., Koenning, M., Jackson, S., Perreau, V.M., Pope, B., Hay, C.M., Mitew, S., Hill, A.F., Lu, Q.R., Wegner, M., Srinivasan, R., Svaren, J., Willingham, M., Barres, B.A., Emery, B., 2013. MYRF is a membrane-associated transcription factor that autoproteolytically cleaves to directly activate myelin genes. PLoS Biol. 11, e1001625. http://dx.doi.org/10.1371/journal.pbio.1001625.

Cartagena, C.M., Ahmed, F., Burns, M.P., Pajoohesh-Ganji, A., Pak, D.T., Faden, A.I., Rebeck, G.W., 2008. Cortical injury increases cholesterol 24S hydroxylase (Cyp46) levels in the rat brain. J. Neurotrauma 25:1087–1098. http://dx.doi.org/10.1089/neu.2007.0444.

Chamelian, L., Reis, M., Feinstein, A., 2004. Six-month recovery from mild to moderate traumatic brain injury: the role of APOE-epsilon4 allele. Brain 127:2621–2628. http://dx.doi.org/10.1093/brain/awh296.

Chrast, R., Saher, G., Nave, K.A., Verheijen, M.H., 2011. Lipid metabolism in myelinating glial cells: lessons from human inherited disorders and mouse models. J. Lipid Res. 52:419–434. http://dx.doi.org/10.1194/jlr.R009761.

Colonna, M., Wang, Y., 2016. TREM2 variants: new keys to decipher Alzheimer disease pathogenesis. Nat. Rev. Neurosci. 17:201–207. http://dx.doi.org/10.1038/nrn.2016.7.

Crawford, F.C., Vanderploeg, R.D., Freeman, M.J., Singh, S., Waisman, M., Michaels, L., Abdullah, L., Warden, D., Lipsky, R., Salazar, A., Mullan, M.J., 2002. APOE genotype influences acquisition and recall following traumatic brain injury. Neurology 58, 1115–1118.

Crawford, F., Wood, M., Ferguson, S., Mathura, V., Gupta, P., Humphrey, J., Mouzon, B., Laporte, V., Margenthaler, E., O'Steen, B., Hayes, R., Roses, A., Mullan, M., 2009. Apolipoprotein E-genotype dependent hippocampal and cortical responses to traumatic brain injury. Neuroscience 159:1349–1362. http://dx.doi.org/10.1016/j.neuroscience.2009.01.033.

Cruchaga, C., Karch, C.M., Jin, S.C., Benitez, B.A., Cai, Y., Guerreiro, R., Harari, O., Norton, J., Budde, J., Bertelsen, S., Jeng, A.T., Cooper, B., Skorupa, T., Carrell, D., Levitch, D., Hsu, S., Choi, J., Ryten, M., Consortium, U.K.B.E., Hardy, J., Ryten, M., Trabzuni, D., Weale, M.E., Ramasamy, A., Smith, C., Sassi, C., Bras, J., Gibbs, J.R., Hernandez, D.G., Lupton, M.K., Powell, J., Forabosco, P., Ridge, P.G., Corcoran, C.D., Tschanz, J.T., Norton, M.C., Munger, R.G., Schmutz, C., Leary, M., Demirci, F.Y., Bamne, M.N., Wang, X., Lopez, O.L., Ganguli, M., Medway, C., Turton, J., Lord, J., Braae, A., Barber, I., Brown, K., Alzheimer's Research, U.K.C., Passmore, P., Craig, D., Johnston, J., McGuinness, B., Todd, S., Heun, R., Kolsch, H., Kehoe, P.G., Hooper, N.M., Vardy, E.R., Mann, D.M., Pickering-Brown, S., Brown, K., Kalsheker, N., Lowe, J., Morgan, K., David Smith, A., Wilcock, G., Warden, D., Holmes, C., Pastor, P., Lorenzo-Betancor, O., Brkanac, Z., Scott, E., Topol, E., Morgan, K., Rogaeva, E., Singleton, A.B., Hardy, J., Kamboh, M.I., St George-Hyslop, P., Cairns, N., Morris, J.C., Kauwe, J.S., Goate, A.M., 2014. Rare coding variants in the phospholipase D3 gene confer risk for Alzheimer's disease. Nature 505:550–554. http://dx.doi.org/10.1038/nature12825.

Dalgard, C.L., Cole, J.T., Kean, W.S., Lucky, J.J., Sukumar, G., McMullen, D.C., Pollard, H.B., Watson, W.D., 2012. The cytokine temporal profile in rat cortex after controlled cortical impact. Front. Mol. Neurosci. 5, 6.

Diaz-Arrastia, R., Gong, Y., Fair, S., Scott, K.D., Garcia, M.C., Carlile, M.C., Agostini, M.A., Van Ness, P.C., 2003. Increased risk of late posttraumatic seizures associated with inheritance of APOE epsilon4 allele. Arch. Neurol. 60:818–822. http://dx.doi.org/10.1001/archneur.60.6.818.

Draper, K., Ponsford, J., 2008. Cognitive functioning ten years following traumatic brain injury and rehabilitation. Neuropsychology 22:618–625. http://dx.doi.org/10.1037/0894-4105.22.5.618.

Ferreira, L.C.B., Regner, A., Miotto, K.D.L., Sd, Moura, Ikuta, N., Vargas, A.E., Chies, J.A.B., Simon, D., 2014. Increased levels of interleukin-6, −8 and −10 are associated with fatal outcome following severe traumatic brain injury. Brain Inj. 28, 1311–1316.

Fitz, N.F., Cronican, A., Pham, T., Fogg, A., Fauq, A.H., Chapman, R., Lefterov, I., Koldamova, R., 2010. Liver X receptor agonist treatment ameliorates amyloid pathology and memory deficits caused by high-fat diet in APP23 mice. J. Neurosci. 30, 6862–6872.

Fitz, N.F., Cronican, A.A., Saleem, M., Fauq, A.H., Chapman, R., Lefterov, I., Koldamova, R., 2012. Abca1 deficiency affects Alzheimer's disease-like phenotype in human ApoE4 but not in ApoE3-targeted replacement mice. J. Neurosci. 32:13125–13136. http://dx.doi.org/10.1523/jneurosci.1937-12.2012.

Fitz, N.F., Cronican, A.A., Lefterov, I., Koldamova, R., 2013. Comment on "ApoE-directed therapeutics rapidly clear beta-amyloid and reverse deficits in AD mouse models". Science 340:924-c. http://dx.doi.org/10.1126/science.1235809.

Fitz, N.F., Tapias, V., Cronican, A.A., Castranio, E.L., Saleem, M., Carter, A.Y., Lefterova, M., Lefterov, I., Koldamova, R., 2015. Opposing effects of Apoe/Apoa1 double deletion on amyloid-beta pathology and cognitive performance in APP mice. Brain 138: 3699–3715. http://dx.doi.org/10.1093/brain/awv293.

Forsyth, S., Horvath, A., Coughlin, P., 2003. A review and comparison of the murine alpha1-antitrypsin and alpha1-antichymotrypsin multigene clusters with the human clade a serpins. Genomics 81, 336–345.

Ghroubi, S., Feki, I., Chelly, H., Elleuch, M.H., 2016. Neuropsychological and behavioral disorders and their correlations with the severity of the traumatic brain injury. Ann. Phys. Rehabil. Med. 59S:e134–e135. http://dx.doi.org/10.1016/j.rehab.2016.07.302.

Guan, F., Gu, J., Hu, F., Zhu, Y., Wang, W., 2012. Association between alpha1-antichymotrypsin signal peptide -15A/T polymorphism and the risk of Alzheimer's disease: a meta-analysis. Mol. Biol. Rep. 39:6661–6669. http://dx.doi.org/10.1007/s11033-012-1472-8.

Gyoneva, S., Ransohoff, R.M., 2015. Inflammatory reaction after traumatic brain injury: therapeutic potential of targeting cell-cell communication by chemokines. Trends Pharmacol. Sci. 36, 471–480.

Haile, Y., Carmine-Simmen, K., Olechowski, C., Kerr, B., Bleackley, R.C., Giuliani, F., 2015. Granzyme B-inhibitor serpina3n induces neuroprotection in vitro and in vivo. J. Neuroinflammation 12:157. http://dx.doi.org/10.1186/s12974-015-0376-7.

Hickman, S.E., Kingery, N.D., Ohsumi, T.K., Borowsky, M.L., Wang, L.C., Means, T.K., El Khoury, J., 2013. The microglial sensome revealed by direct RNA sequencing. Nat. Neurosci. 16:1896–1905. http://dx.doi.org/10.1038/nn.3554.

Holmin, S., Mathiesen, T., Shetye, J., Biberfeld, P., 1995. Intracerebral inflammatory response to experimental brain contusion. Acta Neurochir. 132, 110–119.
Hooli, B.V., Lill, C.M., Mullin, K., Qiao, D., Lange, C., Bertram, L., Tanzi, R.E., 2015. PLD3 gene variants and Alzheimer's disease. Nature 520:E7–E8. http://dx.doi.org/10.1038/nature14040.
Hsu, I., Parkinson, L.G., Shen, Y., Toro, A., Brown, T., Zhao, H., Bleackley, R.C., Granville, D.J., 2014. Serpina3n accelerates tissue repair in a diabetic mouse model of delayed wound healing. Cell Death Dis. 5, e1458. http://dx.doi.org/10.1038/cddis.2014.423.
Hua, F., Wang, J., Ishrat, T., Wei, W., Atif, F., Sayeed, I., Stein, D.G., 2011. Genomic profile of toll-like receptor pathways in traumatically brain-injured mice: effect of exogenous progesterone. J. Neuroinflammation 8, 42.
Jay, T.R., Miller, C.M., Cheng, P.J., Graham, L.C., Bemiller, S., Broihier, M.L., Xu, G., Margevicius, D., Karlo, J.C., Sousa, G.L., Cotleur, A.C., Butovsky, O., Bekris, L., Staugaitis, S.M., Leverenz, J.B., Pimplikar, S.W., Landreth, G.E., Howell, G.R., Ransohoff, R.M., Lamb, B.T., 2015. TREM2 deficiency eliminates TREM2+ inflammatory macrophages and ameliorates pathology in Alzheimer's disease mouse models. J. Exp. Med. 212:287–295. http://dx.doi.org/10.1084/jem.20142322.
Jordan, B.D., 2007. Genetic influences on outcome following traumatic brain injury. Neurochem. Res. 32:905–915. http://dx.doi.org/10.1007/s11064-006-9251-3.
Jordan, B.D., 2014. Chronic traumatic encephalopathy and other long-term sequelae. Continuum (Minneap Minn) 20:1588–1604. http://dx.doi.org/10.1212/01.CON.0000458972.94013.e1.
Kamboh, M.I., Sanghera, D.K., Ferrell, R.E., DeKosky, S.T., 1995. APOE*4-associated Alzheimer's disease risk is modified by alpha 1-antichymotrypsin polymorphism. Nat. Genet. 10:486–488. http://dx.doi.org/10.1038/ng0895-486.
Kawabori, M., Kacimi, R., Kauppinen, T., Calosing, C., Kim, J.Y., Hsieh, C.L., Nakamura, M.C., Yenari, M.A., 2015. Triggering receptor expressed on myeloid cells 2 (TREM2) deficiency attenuates phagocytic activities of microglia and exacerbates ischemic damage in experimental stroke. J. Neurosci. 35:3384–3396. http://dx.doi.org/10.1523/JNEUROSCI.2620-14.2015.
Kelley, B.J., Lifshitz, J., Povlishock, J.T., 2007. Neuroinflammatory responses after experimental diffuse traumatic brain injury. J. Neuropathol. Exp. Neurol. 66, 989–1001.
Kim, J., Basak, J.M., Holtzman, D.M., 2009. The role of apolipoprotein E in Alzheimer's disease. Neuron 63:287–303. http://dx.doi.org/10.1016/j.neuron.2009.06.026.
Lau, D.H., Hogseth, M., Phillips, E.C., O'Neill, M.J., Pooler, A.M., Noble, W., Hanger, D.P., 2016. Critical residues involved in tau binding to fyn: implications for tau phosphorylation in Alzheimer's disease. Acta Neuropathol. Commun. 4:49. http://dx.doi.org/10.1186/s40478-016-0317-4.
Lefterov, I., Fitz, N.F., Cronican, A.A., Fogg, A., Lefterov, P., Kodali, R., Wetzel, R., Koldamova, R., 2010. Apolipoprotein A-I deficiency increases cerebral amyloid angiopathy and cognitive deficits in APP/PS1DeltaE9 mice. J. Biol. Chem. 285, 36945–36957.
Mannix, R.C., Zhang, J., Park, J., Zhang, X., Bilal, K., Walker, K., Tanzi, R.E., Tesco, G., Whalen, M.J., 2011. Age-dependent effect of apolipoprotein E4 on functional outcome after controlled cortical impact in mice. J. Cereb. Blood Flow Metab. 31:351–361. http://dx.doi.org/10.1038/jcbfm.2010.99.
Mannix, R.C., Zhang, J., Park, J., Zhang, X., Bilal, K., Walker, K., Tanzi, R.E., Tesco, G., Whalen, M.J., 2016. Age-dependent effect of apolipoprotein E4 on functional outcome after controlled cortical impact in mice. J. Cereb. Blood Flow Metab. 31, 351–361.
McKee, A.C., Cairns, N.J., Dickson, D.W., Folkerth, R.D., Keene, C.D., Litvan, I., Perl, D.P., Stein, T.D., Vonsattel, J.P., Stewart, W., Tripodis, Y., Crary, J.F., Bieniek, K.F., Dams-O'Connor, K., Alvarez, V.E., Gordon, W.A., group TC, 2016. The first NINDS/NIBIB consensus meeting to define neuropathological criteria for the diagnosis of chronic traumatic encephalopathy. Acta Neuropathol. 131:75–86. http://dx.doi.org/10.1007/s00401-015-1515-z.
Mootha, V.K., Lepage, P., Miller, K., Bunkenborg, J., Reich, M., Hjerrild, M., Delmonte, T., Villeneuve, A., Sladek, R., Xu, F., Mitchell, G.A., Morin, C., Mann, M., Hudson, T.J., Robinson, B., Rioux, J.D., Lander, E.S., 2003. Identification of a gene causing human cytochrome c oxidase deficiency by integrative genomics. Proc. Natl. Acad. Sci. U. S. A. 100:605–610. http://dx.doi.org/10.1073/pnas.242716699.
Moran, L., Taylor, H., Ganesalingam, K., Gastier-Foster, J., Frick, J., Bangert, B., Dietrich, A., Nuss, K., Rusin, J., Wright, M., Yeates, K., 2009. Apolipoprotein E4 as a predictor of outcomes in pediatric mild traumatic brain injury. J. Neurotrauma 26, 1489–1495.
Morganti, J.M., Jopson, T.D., Liu, S., Riparip, L.-K., Guandique, C.K., Gupta, N., Ferguson, A.R., Rosi, S., 2015. CCR2 antagonism alters brain macrophage polarization and ameliorates cognitive dysfunction induced by traumatic brain injury. J. Neurosci. 35, 748–760.
Nam, K.N., Mounier, A., Fitz, N.F., Wolfe, C., Schug, J., Lefterov, I., Koldamova, R., 2016. RXR controlled regulatory networks identified in mouse brain counteract deleterious effects of Abeta oligomers. Sci. Rep. 6:24048. http://dx.doi.org/10.1038/srep24048.
Nygaard, H.B., van Dyck, C.H., Strittmatter, S.M., 2014. Fyn kinase inhibition as a novel therapy for Alzheimer's disease. Alzheimers Res. Ther. 6:8. http://dx.doi.org/10.1186/alzrt238.
Osisami, M., Ali, W., Frohman, M.A., 2012. A role for phospholipase D3 in myotube formation. PLoS One 7, e33341. http://dx.doi.org/10.1371/journal.pone.0033341.
Panicker, N., Saminathan, H., Jin, H., Neal, M., Harischandra, D.S., Gordon, R., Kanthasamy, K., Lawana, V., Sarkar, S., Luo, J., Anantharam, V., Kanthasamy, A.G., Kanthasamy, A., 2015. Fyn kinase regulates microglial neuroinflammatory responses in cell culture and animal models of Parkinson's disease. J. Neurosci. 35:10058–10077. http://dx.doi.org/10.1523/JNEUROSCI.0302-15.2015.
Perez-Garcia, G., Gama Sosa, M.A., De Gasperi, R., Lashof-Sullivan, M., Maudlin-Jeronimo, E., Stone, J.R., Haghighi, F., Ahlers, S.T., Elder, G.A., 2016. Chronic post-traumatic stress disorder-related traits in a rat model of low-level blast exposure. Behav. Brain Res. http://dx.doi.org/10.1016/j.bbr.2016.09.061.
Ponsford, J., Draper, K., Schonberger, M., 2008. Functional outcome 10 years after traumatic brain injury: its relationship with demographic, injury severity, and cognitive and emotional status. J. Int. Neuropsychol. Soc. 14:233–242. http://dx.doi.org/10.1017/S1355617708080272.
Richter, F., Gao, F., Medvedeva, V., Lee, P., Bove, N., Fleming, S.M., Michaud, M., Lemesre, V., Patassini, S., De La Rosa, K., Mulligan, C.K., Sioshansi, P.C., Zhu, C., Coppola, G., Bordet, T., Pruss, R.M., Chesselet, M.F., 2014. Chronic administration of cholesterol oximes in mice increases transcription of cytoprotective genes and improves transcriptome alterations induced by alpha-synuclein overexpression in nigrostriatal dopaminergic neurons. Neurobiol. Dis. 69:263–275. http://dx.doi.org/10.1016/j.nbd.2014.05.012.
Rodriguez, G.A., Burns, M.P., Weeber, E.J., Rebeck, G.W., 2013. Young APOE4 targeted replacement mice exhibit poor spatial learning and memory, with reduced dendritic spine density in the medial entorhinal cortex. Learn. Mem. 20:256–266. http://dx.doi.org/10.1101/lm.030031.112.
Rolls, A., Shechter, R., Schwartz, M., 2009. The bright side of the glial scar in CNS repair. Nat. Rev. Neurosci. 10:235–241. http://dx.doi.org/10.1038/nrn2591.
Saber, M., Kokiko-Cochran, O., Puntambekar, S.S., Lathia, J.D., Lamb, B.T., 2016. Triggering receptor expressed on myeloid cells 2 deficiency alters acute macrophage distribution and improves recovery after traumatic brain injury. J. Neurotrauma http://dx.doi.org/10.1089/neu.2016.4401.
Saher, G., Stumpf, S.K., 2015. Cholesterol in myelin biogenesis and hypomyelinating disorders. Biochim. Biophys. Acta 1851:1083–1094. http://dx.doi.org/10.1016/j.bbalip.2015.02.010.
Saher, G., Brugger, B., Lappe-Siefke, C., Mobius, W., Tozawa, R., Wehr, M.C., Wieland, F., Ishibashi, S., Nave, K.A., 2005. High cholesterol level is essential for myelin membrane growth. Nat. Neurosci. 8:468–475. http://dx.doi.org/10.1038/nn1426.
Savage, J.C., Jay, T., Goduni, E., Quigley, C., Mariani, M.M., Malm, T., Ransohoff, R.M., Lamb, B.T., Landreth, G.E., 2015. Nuclear receptors license phagocytosis by trem2+ myeloid cells in mouse models of Alzheimer's disease. J. Neurosci. 35:6532–6543. http://dx.doi.org/10.1523/JNEUROSCI.4586-14.2015.
Schiza, N., Sargiannidou, I., Kagiava, A., Karaiskos, C., Nearchou, M., Kleopa, K.A., 2015. Transgenic replacement of Cx32 in gap junction-deficient oligodendrocytes rescues the phenotype of a hypomyelinating leukodystrophy model. Hum. Mol. Genet. 24:2049–2064. http://dx.doi.org/10.1093/hmg/ddu725.
Subramanian, A., Tamayo, P., Mootha, V.K., Mukherjee, S., Ebert, B.L., Gillette, M.A., Paulovich, A., Pomeroy, S.L., Golub, T.R., Lander, E.S., Mesirov, J.P., 2005. Gene set enrichment analysis: a knowledge-based approach for interpreting genome-wide expression profiles. Proc. Natl. Acad. Sci. U. S. A. 102:15545–15550. http://dx.doi.org/10.1073/pnas.0506580102.
Tsai, P.C., Yang, D.M., Liao, Y.C., Chiu, T.Y., Kuo, H.C., Su, Y.P., Guo, Y.C., Soong, B.W., Lin, K.P., Liu, Y.T., Lee, Y.C., 2016. Clinical and biophysical characterization of 19 GJB1 mutations. Ann. Clin. Transl. Neurol. 3:854–865. http://dx.doi.org/10.1002/acn3.347.
Venables, W.N., Ripley, B.D., 2002. Modern Applied Statistics with S. Statistics and Computing. fourth ed. Springer-Verlag, New York.
Wang, C., Tan, L., Wang, H.F., Yu, W.J., Liu, Y., Jiang, T., Tan, M.S., Hao, X.K., Zhang, D.Q., Yu, J.T., Alzheimer's Disease Neuroimaging, I., 2015. Common variants in PLD3 and correlation to amyloid-related phenotypes in Alzheimer's disease. J. Alzheimers Dis. 46:491–495. http://dx.doi.org/10.3233/JAD-150110.
Wang, Y., Cella, M., Mallinson, K., Ulrich, J.D., Young, K.L., Robinette, M.L., Gilfillan, S., Krishnan, G.M., Sudhakar, S., Zinselmeyer, B.H., Holtzman, D.M., Cirrito, J.R., Colonna, M., 2015. TREM2 lipid sensing sustains the microglial response in an Alzheimer's disease model. Cell 160:1061–1071. http://dx.doi.org/10.1016/j.cell.2015.01.049.
Washington, P.M., Forcelli, P.A., Wilkins, T., Zapple, D.N., Parsadanian, M., Burns, M.P., 2012. The effect of injury severity on behavior: a phenotypic study of cognitive and emotional deficits after mild, moderate, and severe controlled cortical impact injury in mice. J. Neurotrauma 29:2283–2296. http://dx.doi.org/10.1089/neu.2012.2456.
Whitnall, L., McMillan, T.M., Murray, G.D., Teasdale, G.M., 2006. Disability in young people and adults after head injury: 5-7 year follow up of a prospective cohort study. J. Neurol. Neurosurg. Psychiatry 77:640–645. http://dx.doi.org/10.1136/jnnp.2005.078246.
Willemse-van Son, A.H.P., Ribbers, G.M., Hop, W.C.J., van Duijn, C.M., Stam, H.J., 2008. Association between apolipoprotein-epsilon4 and long-term outcome after traumatic brain injury. J. Neurol. Neurosurg. Psychiatry 79, 426–430.
Yang, S.H., Gangidine, M., Pritts, T.A., Goodman, M.D., Lentsch, A.B., 2013. Interleukin 6 mediates neuroinflammation and motor coordination deficits after mild traumatic brain injury and brief hypoxia in mice. Shock (Augusta, Ga) 40, 471–475.
Yiu, G., He, Z., 2006. Glial inhibition of CNS axon regeneration. Nat. Rev. Neurosci. 7:617–627. http://dx.doi.org/10.1038/nrn1956.
Zhang, B., Horvath, S., 2005. A general framework for weighted gene co-expression network analysis. Stat. Appl. Genet. Mol. Biol. 4 (Article17-Article17).
Zhao, W., Langfelder, P., Fuller, T., Dong, J., Li, A., Hovarth, S., 2010. Weighted gene coexpression network analysis: state of the art. J. Biopharm. Stat. 20:281–300. http://dx.doi.org/10.1080/10543400903572753.